The Fluid Mechanics of Slender Wing Rock

L E Ericsson*
Lockheed Missiles & Space Company, Inc , Sunnyvale California

The limit cycle oscillation in roll of very slender delta wings the so called wing rock is caused by asymmetric vortex shedding from the wing leading edges and not by vortex burst The breakdown or burst of the leading edge vortices of a delta wing can lead to static instability with associated roll divergence Vortex burst however can never be the cause of wing rock because it has a dynamically stabilizing effect on the roll oscillations Consequently slender wing rock is only realized for delta wings with more than 74 deg leading edge sweep in which case vortex asymmetry occurs before vortex breakdown A careful analysis of available experimental data reveals the fluid mechanical process that generates slender wing rock A simple analytic method is formulated by which the experimentally observed limit cycle amplitude in roll can be predicted provided that the static aerodynamic characteristics are known e g from static tests

Nomenclature

b = wing span
c_0 = root chord
d = cylinder diameter
f = frequency of oscillation
ℓ = rolling moment coefficient $C_\ell = \ell/(\rho_\infty U_\infty^2/2)Sb$
M_p = pitching moment, coefficient $C_m = M_p/(\rho_\infty U_\infty^2/2)Sd$
N = normal force coefficient $C_N = N/(\rho_\infty U_\infty^2/2)S$
$C_{NOR} = C_N \cos\phi$
S = reference area wing area or $(\pi d^2/2)$
t = time
T = oscillation period
U = velocity
$\bar{U}$ = convection velocity
x = chordwise distance from apex
α = angle of attack
β = angle of side slip
Δ = increment or amplitude
θ = angular perturbation in pitch
θ_A = apex half angle
θ_{LE} = complimentary angle to the leading edge sweep $\theta_{LE} = \pi/2 - \Lambda$
Λ = leading edge sweep angle
ξ = dimensionless x-coordinate, $\xi = x/c_0$
ρ = air density
ϕ = roll angle
ψ = phase angle $\psi = \omega t$
ω = angular frequency $\omega = 2\pi f$
$\bar{\omega}$ = reduced frequency $\bar{\omega} = \omega c_0/U_\infty$

Subscripts

A = apex
C = critical
eff = effective
F = flare
H = hysteresis
L = left wing half
LE = leading edge
lim = limit cycle
R = right wing half
WR = wing rock
0 = initial or time average value
$1\ 2$ = numbering subscripts
∞ = freestream conditions

Superscripts

i = separation induced e g $\Delta^i C_{N_F}$ in Fig 3
$\bar{()}$ = barred quantities denote integrated mean values e g centroid of aerodynamic loads

Differential Symbols

$\dot{\phi}$ = $\partial\phi/\partial t$
$C_{l\beta}$ = $\partial C_l/\partial\beta$
$C_{l\dot{\phi}}$ = $\partial C_l/\partial(b\dot{\phi}/2U_\infty)$
$C_{m\theta}$ = $\partial C_m/\partial\theta$
$C_{m\dot{\theta}}$ = $\partial C_m/\partial(c\dot{\theta}/U_\infty)$

Introduction

THE steadily increasing demands on performance expose present day aerospace vehicles to unsteady flowfields generating highly nonlinear aerodynamics with significant coupling between longitudinal and lateral degrees of freedom [1 3] The complex vehicle dynamics are caused by separated flow effects of various types which have largely eluded theoretical description Consequently the vehicle designer is dependent upon existing experimental capabilities for dynamic testing [4] where dynamic support interference[5] often adds to the complexity of the separated flow charac teristics Thus it can be rather difficult to obtain a true description of nonlinear pitch yaw roll coupling phenomena such as wing rock and nose slice In the present paper existing experimental results for wing rock of slender delta wings are examined to obtain an understanding of the underlying fluid mechanics

Discussion

Recent systematic experiments performed by Nguyen Yip and Chambers [6] provide the information needed to fully describe the fluid mechanics leading to slender wing rock The phenomenon is similar in many aspects to the limit cycle oscillation in pitch observed on blunt cylinder flare bodies [7 8] Thus the roll oscillations of an 8 deg delta wing are self excited and build up to a limit cycle amplitude[6] (Fig. 1)—an oscillatory behavior very similar to that observed for blunt nosed cylinder flare bodies [7 8] The one degree of freedom oscillation in roll $\phi = -\Delta\phi\sin\omega t$ in Fig 1 induces the following effective angles of attack and sideslip (on each half of the delta wing)

$$\alpha_{EFF} = \arctan(\tan\alpha_0 \cos\phi) \tag{1}$$

$$\beta_{EFF} = \arcsin(\sin\alpha_0 \sin\phi) \tag{2}$$

where $\alpha_0 = \alpha$ at $\phi = 0$

Presented as Paper 82 1320 at the AIAA 9th Atmospheric Flight Mechanics Conference San Diego Calif Aug 9 11 1982; received Sept 18 1983; revision received Dec 13 1983

*Senior Consulting Engineer Fellow AIAA

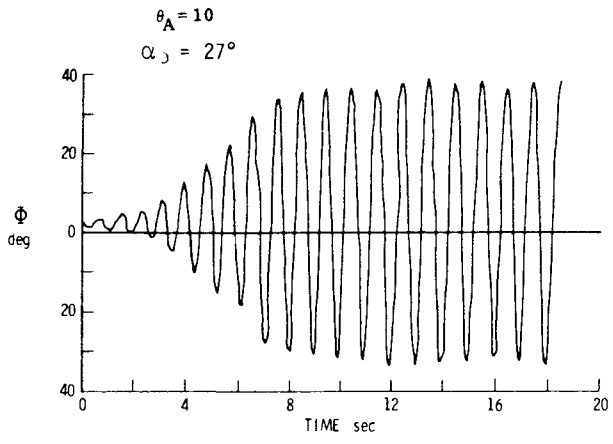

Fig. 1 Time history of wing rock at $\alpha = 27$ deg of an 80 deg delta wing (Ref 6)

The main effect is the induced sideslip Thus one can compare the $C_\ell(\beta)$ characteristics for a slender delta wing[9] (Fig 2a) with the $C_m(\alpha)$ characteristics for a cylinder-flare body (Fig 2b) [8] In both cases the characteristics change in a discontinuous fashion and are likely to be associated with hysteresis both typical behaviors for the effects of separated flow The aerodynamic stiffness $C_{\ell\beta}$ in Fig 2a and $C_{m\alpha}$ in Fig 2b increases dramatically when the discontinuity is encountered (ΔC_ℓ and ΔC_m respectively) Both discontinuous changes of the aerodynamic characteristics are associated with convective time lag effects [7 8 10] This causes the statically stabilizing effects to become dynamically destablizing as is illustrated in Fig 3 for the cylinder flare body The separated shear layer impacting on the flare at time t when $\alpha(t) = 0$ was generated by the nose at a time increment Δt earlier when the angle of attack was $\alpha(t - \Delta t) > 0$ Thus a separation induced residual flare force exists at $\alpha(t) = 0$ which drives the motion and consequently is undamping

When the discontinuity is encountered the damping effect of the separation induced flare force component ($\Delta^i C_{NF}$ in Fig 3) causes divergent oscillations in pitch The amplitude grows until the attached flow damping balances the separation induced negative damping or undamping For $\alpha_0 + \Delta\theta < 9$ deg in Fig 2b the flow is attached to both top and bottom sides of the cylinder flare body † whereas it is at tached only on the bottom side for $\alpha_0 + \Delta\theta > 14$ deg Thus for the body in Fig 2b the limit cycle amplitude—the amplitude for which the separation induced negative damping is equal in magnitude to the positive damping generated by the attached flow—will definitely be larger than 3 deg which is half the extent of the α hysteresis

In reality the limit cycle amplitude is likely to be larger than 10 deg even in absence of any hysteresis effects [7 8] The reason for this is the time lag effect illustrated in Fig 3 and demonstrated by the results in Fig 4 It is shown in Refs 7 and 8 how the unsteady aerodynamics measured for oscillations of large amplitude ($\Delta\theta$) around $\alpha_0 = 0$ can be predicted from static aerodynamic characteristics when ac counting for the convective time lag effect

The separation induced flare force component $\Delta^i C_{NF}$ in Fig 3 generates a negative statically stabilizing, pitching moment discontinuity $\Delta C_m \approx -0\,8$ in Fig 2b Likewise the sudden liftoff of one of the leading edge vortices on the 82 5 deg delta wing in Fig 2a generates a negative statically stabilizing rolling moment discontinuity $\Delta C_\ell \approx -0\,1$ Equation (2) shows that the rolling moment discontinuity will also be encountered when the roll angle ϕ is varied rather than the side slip angle β The sudden change of the leading edge

†The small local flow separation in the cylinder flare juncture has negligible effect

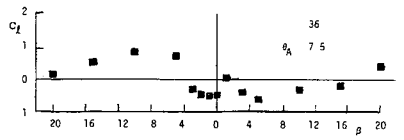

a) $C_\ell(\beta)$ of an 82 5 deg delta wing (Ref 4)

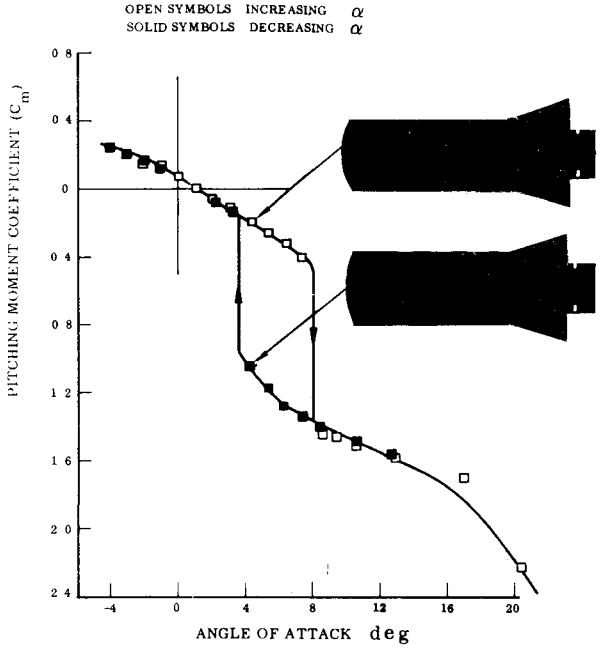

b) $C_m(\alpha)$ of a blunt nosed cylinder flare body (Ref 3)

Fig 2 Nonlinear aerodynamic characteristics

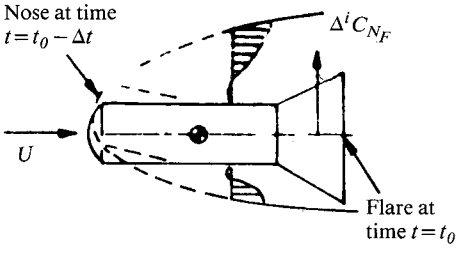

Fig 3 Dynamic effect of time lag

vortex on a delta wing is associated with convected time lag effects as illustrated by the experimentally observed for mation of the leading edge vortex (Fig 5) [10] Accounting for this time lag provides good prediction of the nonlinear vortex induced unsteady aerodynamics of slender delta wings at high angles of attack [11 12] and should also permit the effect of the discontinuous aerodynamics associated with the vortex asymmetry to be predicted

Two types of separation induced discontinuities occur for the slender delta wing One is caused by the breakdown of the leading edge vortices It is the three dimensional equivalent to airfoil stall For very slender delta wings another discon tinuous change of the aerodynamics can occur before vortex breakdown caused by asymmetric leading edge vortices The asymmetric vortex phenomenon has been studied extensively in the case of slender bodies of revolution[13 14] and has been observed also on slender delta wings [15] Vortex asymmetry occurs before vortex breakdown only for very slender delta

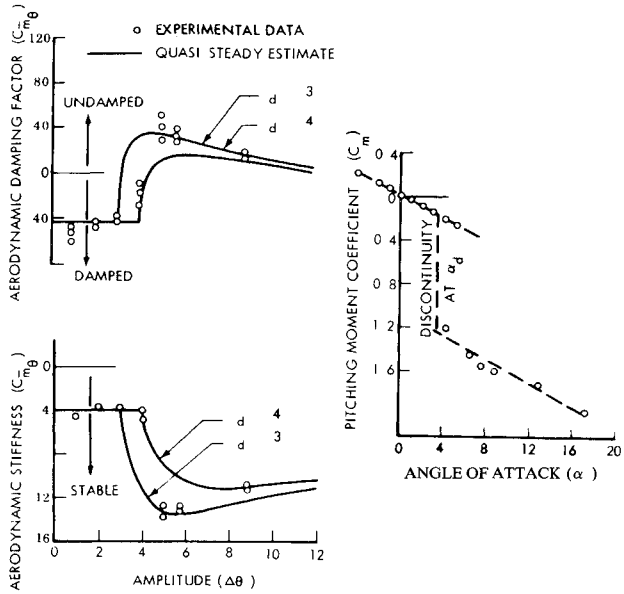

Fig 4 Nonlinear unsteady aerodynamics of a blunt cylinder flare body (Ref 8)

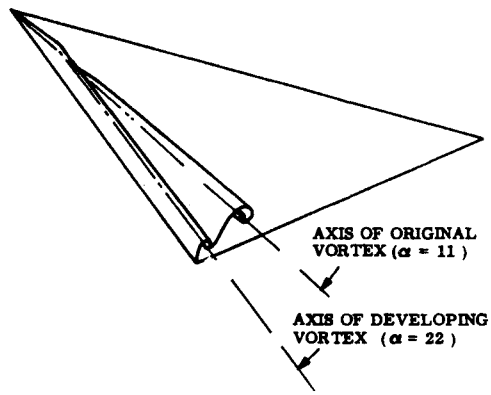

Fig 5 Leading edge vortex formation on a delta wing (Ref 10)

wings $\theta_A < 16$ deg according to experiments (Fig 6) [16,17] In order to use Fig 6 to explore the effects of sideslip β and roll angle ϕ, an effective apex half angle $\bar{\Phi}_A$ is formulated for the right‡ and left‡ wing halfs The following expression is obtained for small angles, ($\theta_A \leq 15$ deg $\beta \leq 15$ deg)

$$\bar{\theta}_A = \theta_A + \Delta\theta_A \tag{3a}$$

$$(\Delta\theta_A)_{RL} = \pm \tan\alpha_0 \sin\phi \tag{3b}$$

$$(\Delta\theta_A)_{RL} = \pm \beta/\cos\alpha_0 \tag{3c}$$

where plus and minus signs refer to right and left wing halves respectively

Experimental results demonstrate that wing rock starts before vortex breakdown and that wing rock is associated with a loss of the time averge lift (Fig 7) [6,18] It is of course to be expected that the liftoff of one of the leading edge vortices[15] will cause a loss of lift Thus wing rock is caused by the vortex asymmetry and not by the vortex breakdown Figures 8 and 9 illustrate the fluid mechanical reasons for this At an $\alpha - \theta_A$ combination where vortex asymmetry occurs the wing half with the lifted off vortex loses lift and dips downs rotating around the roll axis (Fig 8) As a result of the increasing roll angle ϕ the effective apex angle $\bar{\theta}_A$ is increased [Eqs (3a) and (3b)] and the vortex attaches again

‡From a hypothetical pilot s point of view

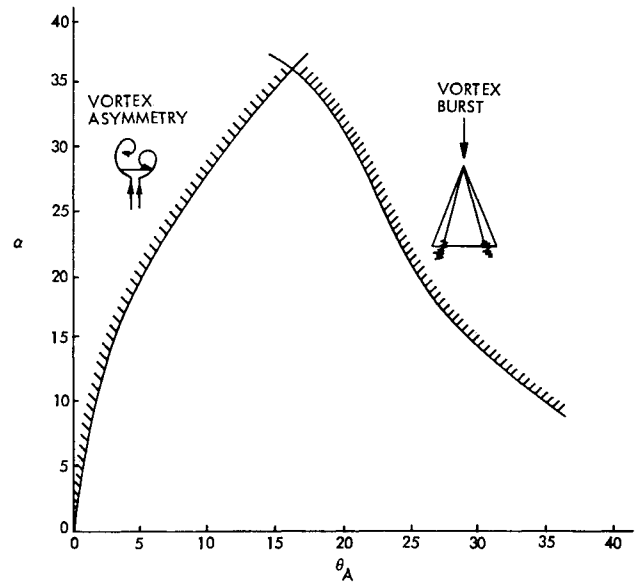

Fig 6 Boundaries for vortex asymmetry and vortex burst (Ref 16)

This produces a restoring rolling moment the positive aerodynamic spring needed for the rigid body§ oscillation in roll (Fig 1) Due to the convective time lag effect discussed earlier the wing is dynamically unstable in roll until the amplitude has reached the limit cycle magnitude At this magnitude the damping on both sides of the discontinuity suffices to balance the undamping as was illustrated by the cylinder flare results in Fig 4 According to Fig 8 for an 80 deg delta wing ($\theta_A = 10$ deg) wing rock should start occurring at $\alpha \approx 27$ deg which is in excellent agreement with experimental results [6]

Thus, the discontinuity introduced by the vortex asymmetry has all the characteristics needed for the limit cycle oscillation in roll Figure 9 demonstrates that these characteristics are lacking in vortex breakdown If for some reason (for example the presence of external disturbances) the vortex burst becomes asymmetric as is sketched in Fig 9 the resulting net loss of lift on one wing half will cause it to ' dip down ' This increases ϕ and thereby $\bar{\theta}_A$ [Eqs (3a) and (3b)], causing the wing half to penetrate further into the vortex burst region No switch to a restoring moment occurs The opposite wing half gets out of the vortex burst region generating increased lift which adds to the statically destabilizing rolling moment

Thus no restoring moment and no positive aerodynamic spring is generated and no rigid body ϕ oscillation is possible If the positive spring is provided by the structure as in the case of elastic vehicle dynamics the dynamic effect of the vortex breakdown would be dynamically stabilizing and damping since the vortex burst is also associated with time lag effects. Thus vortex breakdown has aerodynamic characteristics leading to roll divergence which are completely opposite to those needed to cause slender wing rock

Whereas Nguyen Yip and Chambers[6] measured no wing rock for their 80 deg delta wing below $\alpha = 27$ deg Levin and Katz[18] had already measured wing rock at $\alpha = 20$ deg for the same leading edge sweep (Fig 10) This early wing rock occurrence is probably as the authors suggest caused by the centerbody used in their model (see inset in Fig 10) The smaller limit cycle amplitude ($\Delta\phi \approx 12$ deg compared to $\Delta\phi \approx 34$ deg), which was the limit cycle amplitude measured at $\alpha = 27$ deg (Ref 6), is probably due to the lesser vortex induced loads existing at the lower angle of attack [11]

§In the case of elastic vehicle dynamics the structural stiffness usually ensures a positive spring regardless of the sense of the aerodynamic moment

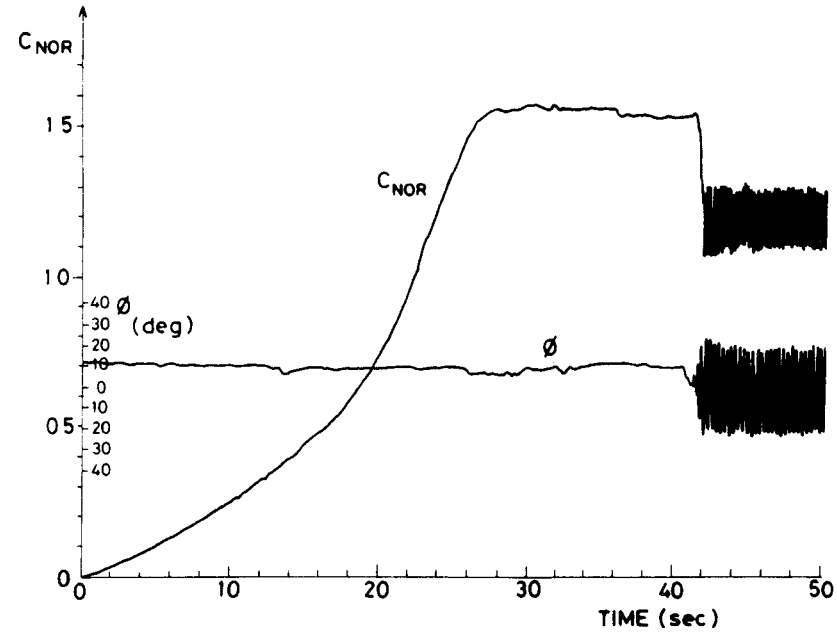

Fig 7 Development of wing rock for an 80 deg delta wing at $\alpha = 35$ deg (Ref 18)

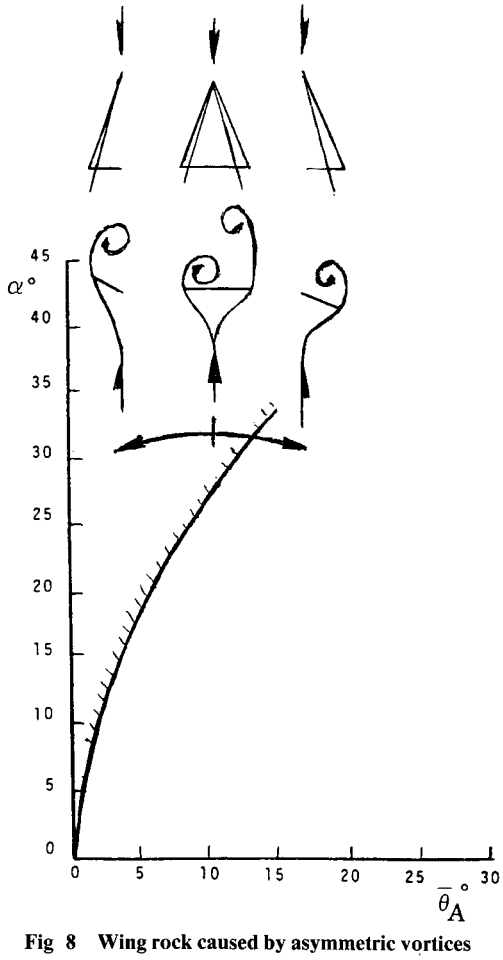

Fig 8 Wing rock caused by asymmetric vortices

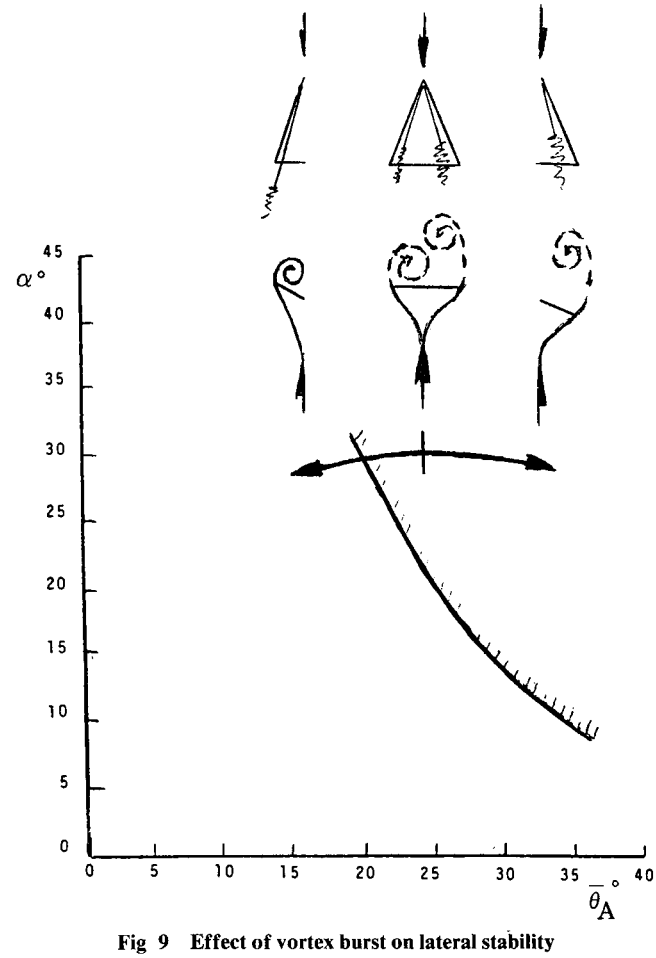

Fig 9 Effect of vortex burst on lateral stability

The oscillations in roll damped down to zero amplitude if the 80 deg delta wing ($\theta_A = 10$ deg) was yawed to $\beta = 10$ deg at $\alpha = 27$ deg (Ref 6) This is, of course to be expeced as the windward wing half has $\tilde{\theta}_A > 15$ deg [Eqs (2) (3a) and (3c)] leaving it outside of the boundary for asymmetric vortex shedding (Fig 8) whereas the leeward wing half with $\tilde{\theta}_A < 5$ deg remains inside the region for vortex asymmetry Thus neither wing half crosses the boundary and the wing rock inducing discontinuity is never encountered

According to Fig 6, no wing rock should occur at $\alpha = 35$ deg if $\theta_A > 16$ deg That is for the 80 deg delta wing in Fig 11 damping should be measured at a $|\beta|$ which gives $\Delta\theta_A > 6$ deg in Eq (3c) i e for $|\beta| > 5$ deg This is in good agreement with the damping characteristics deduced in Ref 6 from the experimental results However Fig 6 also shows that no wing rock should occur at $\alpha = 25$ deg which seems to contradict the results[6] in Fig 11 showing negative damping for $\alpha = 25$ deg at $\beta = 0$ It is true that self excited spontaneous wing rock at

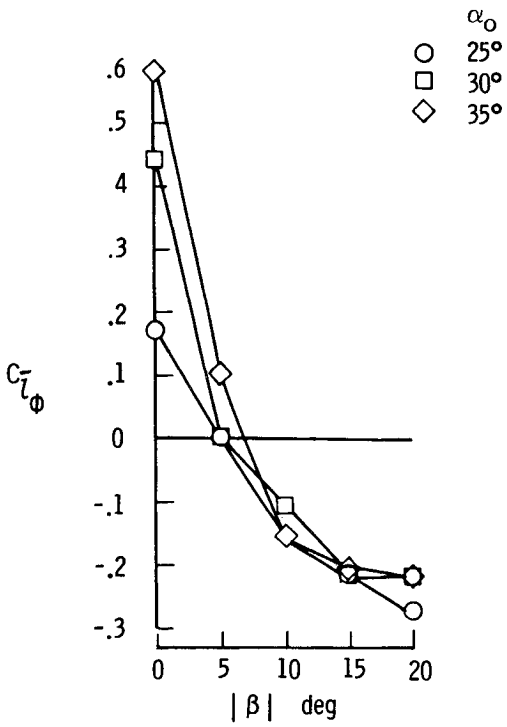

Fig. 10 Effect of side slip of roll damping on an 80-deg delta wing (Ref. 6).

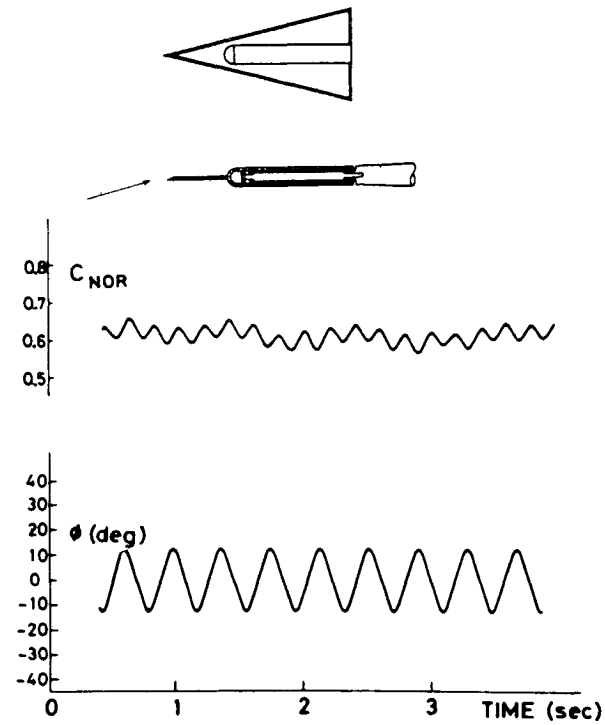

Fig. 11 Time history for wing rock, $\Lambda = 80$ deg, $\beta = 0$, and $\alpha = 20$ deg, (Ref. 18).

$\beta = 0$ was not observed below $\alpha = 27$ deg (see Table 1 of Ref. 6). However, the negative damping in Fig. 11 for $\beta = 0$ was measured in forced oscillations, $\phi = \Delta\phi \sin\omega t$, where $\Delta\phi = 5$ deg. This corresponds to $\Delta\theta_A = 2.35$ deg at $\alpha = 25$ deg, according to Eq. (3b). Thus, the forced oscillations did catch the discontinuity ΔC_ℓ in the rolling moment characteristics, caused by asymmetric vortex liftoff, explaining the measured negative damping.

It was noted by the authors in Ref. 18 that the normal force measured during wing rock was below that measured in static tests. Thus, at $\alpha = 20$ deg the mean- or time-average normal force is $C_{NOR} \approx 0.64$ for $\Delta\phi_{lim} \approx 14$ deg (Fig. 10), whereas the static data showed C_{NOR} to vary from $C_{NOR} \approx 0.80$ to $C_{NOR} \approx 0.65$ when ϕ increased from 0 to 15 deg. Since the static data show no rolling moment at $\beta = \phi = 0$ for $\alpha < 32$ deg, it is obvious that the vortices stayed symmetric in the static case, whereas in the dynamic test vortex asymmetry must have been present to cause the wing rock. The likely reason for this anomaly is the large centerbody Whereas a thin splitter plate of similar height has been found to trigger early vortex asymmetry also in static tests[19] by forcing asymmetric stagnation flow conditions on the topside,[20] the lateral extent of the center body in Ref. 18 apparently allowed symmetric vortex formation in the static test. As a matter of fact, the wing rock motion was not self-induced at $\alpha = 20$ deg. Even at $\alpha = 35$ deg the vortices remained symmetric for 15 s (Fig. 7). Vortex asymmetry cannot, however, explain the big difference observed at $\alpha = 30$ deg, where in the dynamic test, with $\Delta\phi_{lim} \approx 30$ deg, C_{NOR} varied between $C_{NOR} \approx 0.86$ and $C_{NOR} \approx 0.5$, whereas the static test gave $C_{NOR} = 1.28$ and $C_{NOR} = 0.8$ for $\phi = 0$ and $\phi = 30$ deg, respectively In other words, the time-average normal force measured in the dynamic test never reached the minimum value $C_{NOR} = 0.8$, indicated by the static test. The likely reason for the additional lift loss is the early vortex burst observed in the dynamic test.[18]

In regard to the use of results in Fig. 6 obtained for symmetric flow conditions, $\beta = \phi = 0$, for the asymmetric flow conditions discussed in Figs. 8 and 9 the following needs to be said. Whereas vortex burst is relatively unaffected by the presence or absence of the vortex on the opposite wing half, the asymmetric vortex shedding is very dependent upon the crowding of the companion vortex. It is the strength of the vortex, represented by α in Fig. 6, and the closeness of the opposite vortex, represented by θ_A in Fig. 6, which together determine whether or not liftoff of the vortex will occur. In a first approximation the effect of side slip on the closeness parameter can be neglected. That is

$$(\theta_A)_{\text{eff}} = [(\theta_A)_L + (\theta_A)_R]/2 \tag{4}$$

It is shown in Ref. 21 that the vortex strength and associated aerodynamic loads are determined by the parameter α/θ_A rather than by α alone. Consequently the indicated changes of θ_A in Fig. 8 should be substituted by changes of $(\alpha/\theta_A)_{\text{eff}}$. That is, the changes would occur in the vertical rather than in the horizontal plane. The conclusion would, however, be the same in regard to the effects of roll angle ϕ.

Analysis

At high angles of attack, where asymmetric vortex liftoff occurs, the rolling moment changes discontinuously at a critical roll angle ϕ_C

$$C_\ell = \begin{cases} C_{\ell_1}(\phi) & |\phi| \le \phi_C \\ C_{\ell_2}(\phi) & |\phi| > \phi_C + \Delta\phi_H \end{cases} \tag{5}$$

$\Delta\phi_H$ represents any occurring hysteresis. For simplicity it will be assumed that $\Delta\phi_H = 0$ in the analysis to follow

The rolling moments $C_{\ell_1}(\phi)$ and $C_{\ell_2}(\phi)$ can be expressed in the following form

$$C_{\ell_1}(\phi) = C_\ell(\alpha) + C_{\ell_{\phi_1}}\phi + C_{\ell_{\dot\phi_1}}\frac{b\phi}{2U_\infty}$$

$$C_{\ell_2}(\phi) = C_\ell(\alpha) + (C_{\ell_{\phi_1}} - C_{\ell_{\phi_2}})\phi_C \tag{6}$$

$$+ C_{\ell_{\phi_2}}\phi + \Delta C_\ell \frac{\phi}{|\phi|} + C_{\ell_{\dot\phi_2}}\frac{b\phi}{2U_\infty}$$

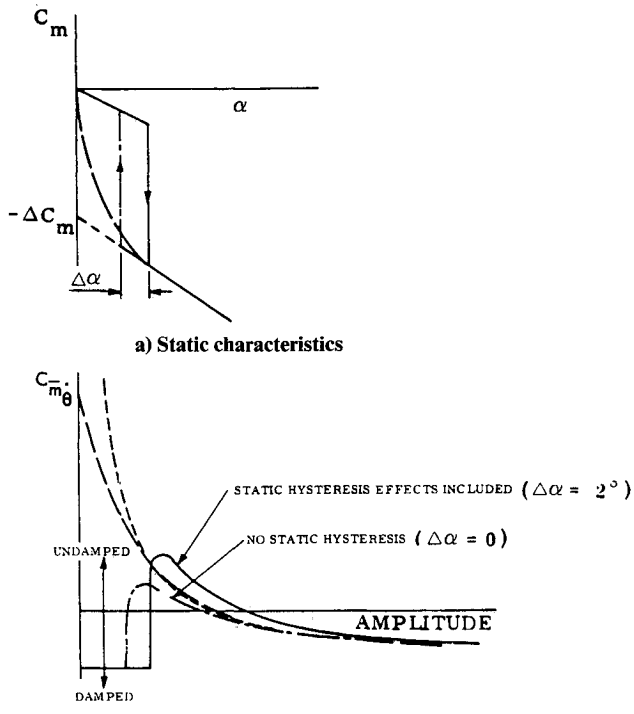

a) Static characteristics

b) Dynamic characteristics

Fig 12 Nonlinear aerodynamic characteristics of blunt cylinder flare bodies (Ref 7)

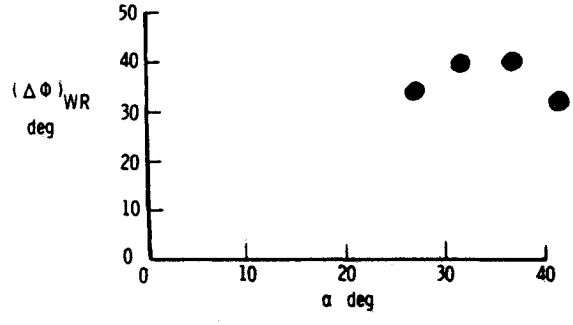

Fig 13 Limit cycle amplitude for roll oscillations of an 80 deg delta wing at $\beta = 0$ (Ref 6)

The vortex induced rolling moment acting at the load center $\bar{x} = c_0\bar{\xi}$ is determined by the roll angle at apex at a time increment Δt earlier where Δt is the time required to convect the vortex change from apex to $\bar{x}$ (Fig 5) That is for sinusoidal oscillations $\phi = \Delta\phi \sin\omega t$

$$\phi_A = \Delta\phi\sin(\omega t - \omega\Delta t) = \Delta\phi\sin(\psi - \Delta\psi)$$
$$\Delta\psi = \omega\Delta t = \omega c_0\bar{\xi}/\bar{U} = \frac{U_\infty}{\bar{U}}\bar{\xi}\bar{\omega} \tag{7}$$

For roll oscillations through the discontinuity ϕ_C an ef fective damping derivative $C_{l_{\bar\phi}}$ can be determined by con sidering the energy dissipation through one cycle of oscillation [7,8]

$$\int_{t_0}^{t_0+T} C_l(t)\,\mathrm{d}\phi = \int_{t_0}^{t_0+T} C_l(t)\,\dot\phi\,\mathrm{d}t = \int_{t_0}^{t_0+T} C_{l_{\bar\phi}}\frac{b\dot\phi}{2U_\infty}\,\dot\phi\,\mathrm{d}t \tag{8}$$

That is

$$C_{l_{\bar\phi}} = \int_{t_0}^{t_0+T} C_l(t)\,\dot\phi\,\mathrm{d}t \Big/ \frac{b}{2U_\infty}\int_{t_0}^{t_0+T}\dot\phi^2\,\mathrm{d}t \tag{9}$$

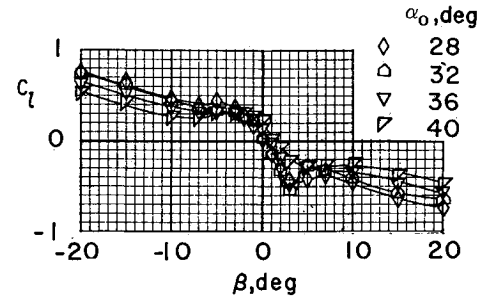

a) Ref 22

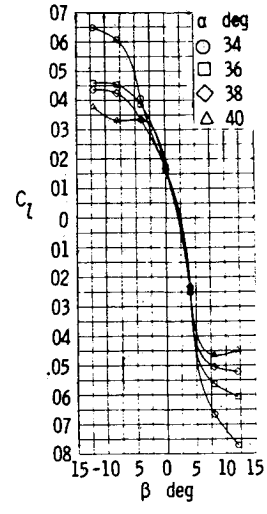

b) Ref 6

Fig 14 Nonlinear rolling moment characteristics of an 80 deg delta wing

Or with $\phi = \Delta\phi\sin\psi$, where $\psi = \omega t$

$$C_{l_{\bar\phi}} = \frac{1}{\pi\Delta\phi}\frac{1}{b\omega/2U_\infty}\int_{\psi_0}^{\psi_0+2\pi} C_l(\psi)\,\mathrm{d}\psi \tag{10}$$

One can combine Eqs (6) (7) and (10) to obtain the following definition of $C_{l_{\bar\phi}}$

$$C_{l_{\bar\phi}} = \frac{2}{\pi\Delta\phi}\frac{1}{b\omega/2U_\infty}\left\{\int_{\Delta\psi}^{\Delta\psi+\psi_1} C_{l_1}\cos\psi\,\mathrm{d}\psi + \int_{\Delta\psi+\psi_1}^{\pi+\Delta\psi-\psi_1}\right.$$
$$\left.\times C_{l_2}\cos\psi\,\mathrm{d}\psi + \int_{\pi+\Delta\psi-\psi_1}^{\pi+\Delta\psi} C_{l_1}\cos\psi\,\mathrm{d}\psi\right\}$$
$$= C_{l_{\dot\phi_2}} - \frac{4}{\pi}\frac{\Delta C_l}{\Delta\phi}\frac{\sin(\bar\omega\bar\xi U_\infty/\bar U)}{b\bar\omega/2c_0} + \frac{2}{\pi}(C_{l_{\dot\phi_1}} - C_{l_{\dot\phi_2}})$$
$$\times\left[\sin^{-1}\left(\frac{\phi_C}{\Delta\phi}\right) - \left(\frac{\phi_C}{\Delta\phi}\right)\sqrt{1-\left(\frac{\phi_C}{\Delta\phi}\right)^2}\cos(2\Delta\psi)\right] \tag{11}$$

A slightly conservative value of the limit cycle amplitude defined by $C_l = 0$, is obtained if the third term is neglected (it would be exactly zero if $C_{l_{\dot\phi_1}} = C_{l_{\dot\phi_2}}$)

$$\Delta\phi_{\lim} = \frac{4}{\pi}\frac{\Delta C_l}{C_{l_{\dot\phi_2}}}\frac{\sin(\bar\omega\bar\xi U_\infty/\bar U)}{b\bar\omega/2c_0} \tag{12}$$

$C_{l_{\dot\phi_2}}$ is the roll damping derivative obtained with symmetric vortices

When approximating Eq (11) by Eq (12), the parameter ϕ_C is eliminated That is it is assumed that it does not matter where the discontinuity occurs in agreement with the results obtained for blunt cylinder flare bodies (Fig 12) [7] The results

in Fig 13 are also in agreement with this conclusion as $\Delta\phi_{\lim}$ varies little when ϕ_C varies from $\phi_C \approx 0$ at $\alpha = 27$ deg to 10 deg or more at $\alpha \leq 37$ deg The variation with α in Fig 13 is ac counted for by the α effect on the vortex strength [21] and thereby on ΔC_ℓ Thus although the values of ϕ_C and $\Delta\phi_H$ are important for computation of the damping characteristics at $\Delta\phi < \Delta\phi_{\lim}$ they can be neglected in a first approximation when determining the limit cycle amplitude as was done in obtaining Eq (12)

For the 80 deg delta wing the roll damping measured at $|\beta| \leq 15$ with only one wing half having the full vortex induced lift was $C_{\ell_{\dot\phi 2}} \approx -0\ 2$ (Ref 6 and Fig 11) As at these high angles of attack the attached flow lift remains prac tically constant [11] one would expect $C_{l_{\dot\phi 2}}$ to approach the value $C_{\ell_{\dot\phi 2}} = -0\ 4$

In addition to $C_{\ell_{\dot\phi 2}}$ one needs to know the value of ΔC_ℓ before Eq (12) can provide an estimate of the limit cycle amplitude For an 82 5 deg delta wing the experimental results[4] in Fig 2a gave $\Delta C_\ell \approx -0\ 1$ For an 80 deg delta wing the $C_\ell(\beta)$ characteristics shown in Fig 14 have been ob tained [6 22] According to Eq (2) one can expect the $C_l(\phi)$ characteristics to have a similar shape Figures 14a and 14b show a steep C_ℓ variation with β through $\beta = 0$ rather than an outright discontinuity Based upon the discussion earlier ΔC_ℓ will be determined the same way ΔC_m was (Fig. 12a) Thus Fig 14 gives $\Delta C_\ell \approx -0\ 08$ for $\Lambda = 80$ deg the delta wing for which the results in Fig 13 were obtained

For the rolling wing the effective α/θ_{LE} variation with ξ is similar to that for a cambered delta wing [23] where local angle of attack is increasing with ξ or a Gothic wing,[24] where θ_{LE} is decreasing with increasing ξ In both cases the vortex induced loads are increasing linearly with increasing ξ Thus the center of the vortex induced loads is located at $\bar\xi = \frac{2}{3}$ rather than at $\bar\xi = 0\ 52$ the $\bar\xi$ value for a delta wing at a constant angle of attack [11 25] Thus $\bar\xi = \frac{2}{3}$ in Eq (12) Experimental results[10 11] indicate that $U_\infty / \bar U = 0\ 75$ The results in Ref 6 were obtained for $\bar\omega = 1\ 12$ With these values Eq (12) gives $\Delta\phi_{\lim} = 0\ 63 = 36$ deg which is in excellent agreement with experimental results (Ref 6 and Fig 13)

Conclusions

An analysis of the slender wing rock phenomenon has shown the following: 1) slender wing rock is caused by asymmetric leading edge vortices 2) vortex breakdown has a damping effect on the roll oscillations and cannot cause wing rock 3) wing rock will only occur for delta wings with more than 74 deg leading edge sweep for which asymmetric vortex formation occurs before vortex burst when the angle of attack is increased and 4) preliminary results indicate that the slender wing rock characteristics can be predicted in an un steady analysis in which the time history effect is represented by a lumped time lag and the static load discontinuity caused by asymmetric vortex liftoff is defined by static experiments

References

[1] Dynamics Stability Parameters AGARD CP 235 Nov 1978

[2] Ericsson, L E Technical Evaluation Report on the Fluid Dynamics Panel Symposium on Dynamic Stability Parameters AGARD AR 137 April 1978

[3] Ericsson L E, A Summary of AGARD FDP Meeting on Dynamic Stability Parameters Paper 2 AGARD CP 260 May 1979

[4] Orlik Rückemann, K J Dynamic Stability Testing of Aircraft Needs Versus Capability Progress Aerospace Science Pergamon Press 1975

[5] Ericsson L E and Reding J P Review of Support In terference in Dynamic Tests *AIAA Journal* Vol 21 Dec 1983 pp 1652 1666

[6] Nguyen L E Yip L P and Chambers J R Self Induced Wing Rock of Slender Delta Wings AIAA Paper 81 1883 Aug 1981

[7] Ericsson L E Unsteady Aerodynamics of Separating and Reattaching Flow on Unsteady Boundary Layers *IUTAM Sym posium* Vol 1 Laval University Quebec May 24 28 1971 pp 575 586

[8] Ericsson L E Separated Flow Effects on the Static and Dynamic Stability of Blunt Nosed Cylinder Flare Bodies NASA CR 76919 Dec 1965

[9] Letko W Experimental Determination at Subsonic Speeds of the Oscillatory and Static Lateral Stability Derivatives of a Series of Delta Wings With Leading Edge Sweep from 30 to 86 5 NACA RM L57A30 April 1957

[10] Lambourne, N C Bryer, D W and Maybrey, J F M The Behavior of the Leading Edge Vortices over a Delta Wing Following a Sudden Change of Incidence R&M No 3645 Aeronautical Research Council Great Britain March 1969

[11] Ericsson L E and Reding J P Unsteady Aerodynamics of Slender Delta Wings at Large Angles of Attack *Journal of Aircraft* Vol. 12 No 9 Sept 1975, pp 721 729

[12] Ericsson L E and Reding J P Unsteady Aerodynamic of Space Shuttle Vehicles Part II: Steady and Unsteady Aerodynamic of Sharp Edged Delta Wings NASA CR 124423 Aug 1973

[13] Ericsson L E and Reding J P Review of Vortex Induced Asymmetric Loads Part I *Z Fluguss* Weltramforsch Vol 5 (1981) Heft 3 pp 162 174

[14] Ericsson L E and Reding J P Review of Vortex Induced Asymmetric Loads Part II *Z Flugwiss* Weltramforsch Vol 5 (1981) Heft 6 pp 369 366

[15] Bird J D, Tuft Grid Surveys at Low Speeds for Delta Wings NASA TND 5045 Feb 1969

[16] Polhamus E C Predictions of Vortex Lift Characteristics by a Leading Edge Suction Analogy *Journal of Aircraft* Vol 8 April 1971 pp 193 199

[17] Johnson J L Jr Grafton S B and Yip L P, Exploratory Investigation of Vortex Bursting on the High Angle of Attack Lateral Directional Stability Characteristics of Highly Swept Wings AIAA Paper 80 0463, March 1980

[18] Levin D and Katz J Dynamic Load Measurements with Delta Wings Undergoing Self Induced Roll Oscillations *Journal of Aircraft* Vol 21 Jan 1984 pp 30 36

[19] Maltby R L et al, 'Low Speed Flow Studies of the Vortex Patterns Above Inclined Slender Bodies Using a New Smoke Technique RAE TN AERO 2482 Nov 1957

[20] Reding J P and Ericsson L E Review of Delta Wing Space Shuttle Vehicle Dynamcis Vol III, *Proceedings of Space Shuttle Aerothermodynamics Conference* NASA Ames Research Center Moffett Field Calif Dec 1971 pp 861 931 (NASA TMX 250)

[21] Ericsson L E and Reding J P Approximate Nonlinear Slender Wing Aerodynamics *Journal of Aircraft* Vol 14 No 12 Dec 1977 pp 1197 1204

[22] Shanks R E Low Subsonic Measurements of Static and Dynamic Stability Derivativs of Six Flat Plate Wings Having Leading Edge Sweep Angles of 70 to 84° NASA TN D 1822 July 1963

[23] Lambourne N C and Bryer D W The Bursting of Leading Edge Vortices Some Observations and Discussion of the Phenomenon R&D No 3282 Aer Res Council Great Britain April 1961

[24] Peckham, D H Low Speed Wind Tunnel Tests on a Series of Uncambered Slender Pointed Wings with Sharp Edges R&M No 3186 Aer Res Council Great Britain Dec 1958

[25] Ericsson L E and Reding, J P Unsteady Aerodynamic Analysis of Space Shuttle Vehicles Part II Steady and Unteady Aerodynamics of Sharp Edged Delta Wings NASA CR 120123 Aug 1973